Available online at www.sciencedirect.com
SCIENCE DIRECT®
Fluid Phase Equilibria 234 (2005) 131–135
FLUID PHASE EQUILIBRIA
www.elsevier.com/locate/fluid

Phase diagram, latent heat, and specific heat of TBAB semiclathrate hydrate crystals

Hiroyuki Oyama, Wataru Shimada, Takao Ebinuma*, Yasushi Kamata, Satoshi Takeya, Tsutomu Uchida, Jiro Nagao, Hideo Narita

National Institute of Advanced Industrial Science and Technology (AIST), Tsukisamu-higashi, Sapporo 062-8517, Japan

Received 24 December 2003; received in revised form 10 May 2005; accepted 15 June 2005

Abstract

Tetra-*n*-butyl ammonium bromide (TBAB) is a tetra-alkylammonium salt, that forms two types of semiclathrate hydrate. At atmospheric pressure, the melting points are between room temperature and freezing point of water. There are some useful applications of the semiclathrate, for example using as a heat transport medium and gas separator, but there are little knowledge about TBAB hydrates characteristics. In this paper, some thermal properties of TBAB semiclathrate hydrate are reported. We determined the phase diagram of semiclathrate hydrate nucleation under the condition of atmospheric pressure, latent and specific heats capacity of TBAB semiclathrate hydrate. From the phase diagram, the congruent melting points of two TBAB hydrates were determined. Using above results, we obtained the hydration numbers of two type TBAB hydrates.

Keywords: Tetra-*n*-butyl ammonium bromide (TBAB); Semiclathrate hydrate; Data; Latent heat; Specific heat; Hydration number; Solid-fluid equilibria

1. Introduction

Thermodynamic studies of tetra-alkylammonium salts in aqueous solution, including tetra-*n*-butyl ammonium bromide (TBAB: $(C_4H_9)_4NBr$), have only recently been done [1–4]. Their unique properties are attributed to the interactions that occur between the hydrophobic alkyl groups of the ions and the water molecules. Tetra-*n*-butylammonium and tetra-isoamylammonium compounds form semiclathrate hydrate crystals below ambient temperature at atmospheric pressure. As most clathrate hydrate crystals require high pressure, the fact that these compounds form semiclathrate hydrate at low pressure suggests that the ammonium ions with long alkyl chains have a strong tendency to enable the surrounding water molecules to form clathrate-like structures even in aqueous solution [1,5]. Though the gas hydrates have been variously studied in recent year, the unclear points are abounding on structure and property for the semiclathrate hydrate.

TBAB also forms a semiclathrate hydrate crystal with water molecules, hereafter called TBAB hydrate, even at atmospheric pressure and at near room temperature. There are some possible applications of the semiclathrate. For example, Fukushima et al. proposed using TBAB hydrate slurry as a heat transport medium [4], and we showed the TBAB hydrate should be useful for separation of gas molecules by their molecular size [6,7]. In the pure system, TBAB hydrate has empty dodecahedral cages. We found that small molecules such as methane, nitrogen, and hydrogen sulfide are selectively encaged in these small cages. However, little is known about TBAB hydrate. In particular, the thermophysical properties that are needed for industrial applications, as mentioned above, are uncertain. Thus, we did thermal measurements of TBAB hydrate in atmospheric pressure in contact with air. We describe the phase diagram and our measurements of the latent and specific heats of TBAB hydrate crystals. The phase diagram was measured more in detail than our previous work [6]. In addition, we determined the hydration numbers

* Corresponding author. Tel.: +81 118551705; fax: +81 118551705.
E-mail addresses: mhdhiro@poppy.ocn.ne.jp (H. Oyama); t.ebinuma@aist.go.jp (T. Ebinuma).

0378-3812/$ – see front matter © 2005 Elsevier B.V. All rights reserved.
doi:10.1016/j.fluid.2005.06.005

of TBAB hydrates. The hydration numbers are important information to determine the semiclathrates crystal structure.

2. Experiment

In our previous study [6], we found that two types of TBAB hydrate can grow simultaneously in aqueous solution, types A and B. When one type of TBAB hydrate nucleates and grows, the concentration of the aqueous solution changes. This makes it difficult to study both types simultaneously. Therefore, it is necessary to measure the thermophysical properties of each TBAB hydrate individually. We did two kinds of experiments to determine the phase change conditions.

We measured the latent and specific heats of each TBAB hydrate crystal by differential scanning calorimeter (DSC). The samples were made by cooling a solution that was made by dissolving TBAB powder (purity 99.8%) into distilled water. The details of measuring methods are described next.

2.1. Phase diagram

Because there are two types of TBAB hydrates in contact with TBAB aqueous solution, there are two melting points for each concentration of TBAB aqueous solution. The DSC curve will contain both melting peaks convoluted, and these peaks are difficult to separate because they are close and mixed together. Thus, it is difficult to determine the phase change temperatures of both types of TBAB hydrates by using one DSC. Hence we used two different techniques to identify the higher and lower temperature melting points separately.

The higher temperature melting point was measured using an autoclave. The reaction vessel was made of stainless steel with an internal volume of 1.3×10^{-3} m^3 and was equipped with a magnetic stirrer and a type T thermocouple. This equipment appropriated for the gas hydrate measurement, and the details is described in our previous paper [8]. We prepared the desired concentration of TBAB solution and then put it in the vessel. The temperature was controlled by circulating brine in a jacket around the vessel.

TBAB hydrates were formed by cooling the sample below the melting temperatures. Then, the temperature was raised at constant heating rate of 2.0 °C/h. The brine fluid was heated so that the sample fluid would be warmed at the rate of 2.0 °C/h if no phase changes occurred. However, the TBAB solution was cooled by the absorption of latent heat as the semiclathrate hydrates were dissolving. After all TBAB hydrates dissolved, the solution temperature rose directly with the brine temperature at a rate of about 2.0 °C/h. The inflection points of the temperature curves marked the phase change points. Thus, when the solution temperature began to rise at a rate of about 2.0 °C/h, it was considered that the solution temperature equalled with the higher melting temperature.

To determine the lower melting temperature of the other hydrate phase, we grew TBAB hydrate crystals using the same method as that reported in our previous paper [6]. Crystals of type A were grown with a 40.0 wt.% concentration of TBAB in solution at 11.0 °C whereas type B crystals were grown with a 10.0 wt.% solution at 5.8 °C. Both samples were grown in the reaction vessel described above. These samples were put into the crystal growth cell with TBAB solution at a concentration of determining the melting point, and the crystal surface was observed using a microscope. The cell volume was 7.7 cm^3; the effective diameter of the window was 35.0 mm. The apparatus over view are described in our previous work [9]. During each measurement, we used sample volumes of solution to ensure that there were no influences from the latent heat of melting and concentration changes due to crystal dissolution. The solution temperature was controlled by circulating brine around the growth cell and measured by a type T thermocouple. The temperature was raised in stepwise of 0.1 °C. To view the crystals, we used a digital CCD microscope (KEYENCE, VH-7000). When the crystal began to dissolve, the surface became visibly rough. This temperature was then identified as the lower melting temperature.

All thermocouples were calibrated against a thermistor sensor (Techno Seven, models SXK-67 and -33 with D641 temperature tracer; accuracy 0.01 K).

2.2. Latent and specific heats

For measuring the latent and specific heats, we grew the sample crystals under conditions in which only one type grew, using the same conditions of lower melting temperature measurement. The crystals were then removed from the cell as was the solution that remained on the surface. The paper filter was used remove the remained water which adhered to the crystals. After remained water was removed, the crystals were quenched in the liquid nitrogen to stabilize. However, the ice might be remained on the type B surface, because they were made at the low concentration solution. The TBAB hydrate crystals were ground to fine powder and stored at liquid nitrogen temperature.

For the measurements, we used a differential scanning calorimeter (DSC) (MAC Science, DSC-3200S). The lowest temperature measurements were done by putting a liquid nitrogen-filled dewar over the sample holder. For temperature and latent heat calibration, we used indium (purity 99.999%) and distilled water. The specific heat capacity data were obtained relative to an external, standard aluminum oxide (α-alumina) powder. The samples were contained in closed aluminum planchets and weights were set at ranging from 2.0 to 5.0 mg. The sample handling and the experiments were done in a cold room at 5.0 °C to prevent crystal decomposition and water condensation on the sample pans. The heating rate was set to 5.0 °C/min, and the measurement temperature range was between −30.0 and 30.0 °C. The final values of specific heat and latent heat were averages of 5–10 measurements.

3. Results and discussion

3.1. Phase diagram

Fig. 1 shows TBAB hydrate crystals, types A and B, that were grown in TBAB aqueous solution of 35.7 wt.% at 9.6 °C. The two types of hydrate have different transmittance, different refraction, and different crystal morphology. Type A has columnar shape and type B has an undefined form composed of thin crystals.

Fig. 2 shows the phase diagram based on our measurements with the autoclave and the microscope observations of the melting temperature. These results were measured well-informed than previous results [6]. Especially, the melting temperature of type B was newly required in the high-concentration part. Near 18 wt.%, the melting curves of these two crystals cross over each other. Type A has the eutectic point at 4.5 wt.%. However, type B does not have a eutectic point. Thus, only type B TBAB hydrate can nucleate at concentrations under 4.5 wt.%. The congruent melting points, defined as the maximum melting temperatures, are about 40 wt.% for type A and about 32 wt.% for type B. The TBAB hydrate hydration numbers were calculated from these congruent melting point concentrations. The calculation formula is a form as:

$$\text{Hydration number} = \frac{(100 - x)/M_{H_2O}}{x/M_{TBAB}}, \quad (1)$$

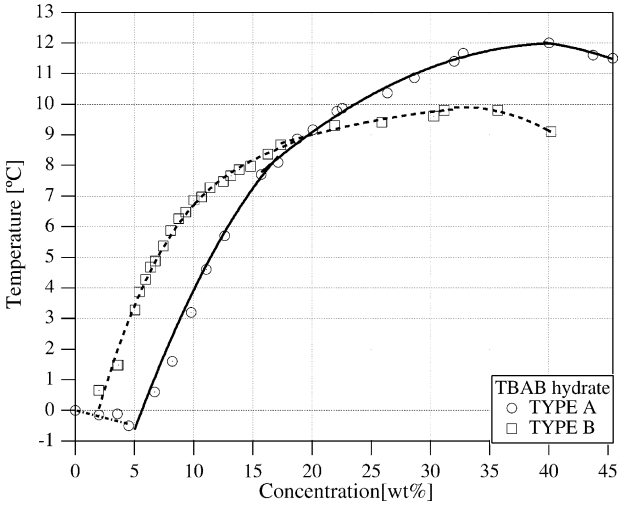

Fig. 2. Phase diagram for TBAB hydrates under atmospheric pressure. The solution was in contact with air. Data are based on both the autoclave and crystal growth results.

where x shows the value of percentage by weight in congruent melting point, M_{H_2O} and M_{TBAB} show water and TBAB molecular weight, respectively. The hydration number is 26.0 for type A and 38.0 for type B.

Table 1 lists the hydration numbers, and the temperature and concentrations at the congruent melting points. The congruent melting points were decided by fitting of

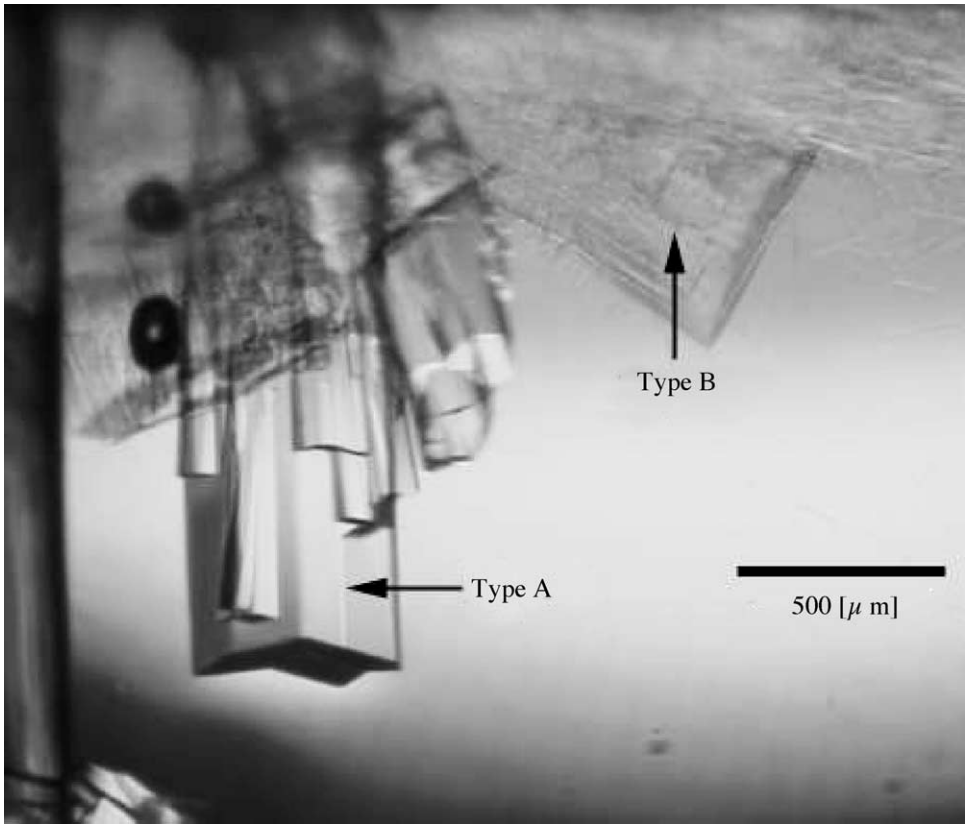

Fig. 1. TBAB semiclathrate hydrates growing in aqueous solution. Both types of hydrates are shown. The conditions are 9.6 °C and 35.7 wt.% TBAB solution.

Table 1
Congruent melting point concentration, melting temperature, and hydration number for both hydrates

Name	Concentration (wt.%)	Melting point (°C)	Hydration number
Type A	40	12.0	26.0
Type B	32	9.9	38.0
Type A[a]	41	11.8	26

[a] From Ref. [4].

the curve and prediction for crystal structures. Possible hydration numbers agreed with these measured value in the consideration using the molecular model. These type A results are consistent with the previous results in Ref. [4]. And it is possible to define the results of type B for the first time.

3.2. Latent heats and specific heats

For measurement of latent heats and specific heats, we used the DSC. As mentioned in Section 2, the using samples for type A measurements were growing at their congruent melting point concentration. On the other hand, since type B samples were not made at the congruent melting point concentration, the ice intermingled with the sample on it. Therefore, we considered that the appeared value in DSC of type B was regarded as linearly combining the value of ice and hydrate. From the melting heat determined from the DSC peak for the melting together with the literature value of specific melting heat of ice, 333.9 J/g. From the total weight of the sample, we subtracted the estimated weight of the ice and assumed that the remaining weight was from type B semi-clathrate hydrate.

In the latent heats measurements, type A samples were measured ten times and type B ones were measured nine times. The resulting dissolution latent heats are 193.18 J/g for type A and 199.59 J/g for type B. The standard deviation becomes 8.52 and 5.28, respectively. Type B one had not been previously measured. Our measured value for type A is close to the value measured in a previous study (193 J/g) [4]. Thus, our calculated type B value has the reliability although which includes the numerical error of estimation.

The specific heats for various temperatures are presented in Table 2. We did not do measurements near the melting points to avoid the singularities. Around the melting point, the values of specific heat would have diverged form dissolution latent heats emission. Thus, we show the result of type A to 10.0 °C and type B to −0.2 °C below ice melting. We measured specific heats seven times and Table 2 results were obtained by fitting to a third-order polynomial function. The function is expressed as:

$$\text{Specific heats} = A + B \times T + C \times T^2 + D \times T^3, \qquad (2)$$

where T is the temperature [K] and A–D, the polynomial coefficients. These coefficients of this function are summarized in Table 3. The measured values examples and fitting results showed in Fig. 3. In these figures, (a) and (b) show types A and B results, respectively. The standard deviation between measured values and fitting results becomes 0.161 J/g K for type A and 0.680 J/g K for type B. From these results, the type A fitting results have small dispersion; on the other hand, the type B fitting results have large dispersion. These differences were caused by the different conditions of samples crystallization. Type A samples were made at congruent melting point, but type B ones were different concentration. Thus, on the surface of type B crystals, there was remained water which could not remove at making the samples. Main part of remained water became ice in which it was quenched at the liquid nitrogen temperature. But there is possibility for the part of water molecules to exist as different hydration form (for example type A). Thus, it is considered that type B dispersions were caused by this influence. However, it is considered that errors are almost being removed by the statistical processing.

From these results, we determined that type B hydrate has a larger latent and specific heats than type A hydrate. This is a consequence of the larger hydration number of type B. Type B apparently requires more energy to dissociate the water molecules that comprise the TBAB hydrate cages. In addi-

Table 3
The coefficients of the fitting function

Coefficient (unit)	Type A	Type B
A (J/g K)	−715.430	−2374.900
B (J/g K^2)	8.044	27.076
C (J/g K^3)	−0.030	−0.103
D (J/g K^4)	3.768×10^{-5}	1.303×10^{-4}

Table 2
TBAB hydrate specific heats at various temperatures

Type A		Type B	
Temperature (°C)	Specific Heat (J/g K)	Temperature (°C)	Specific Heat (J/g K)
−20.0	1.859	−20.0	1.995
−15.0	2.001	−15.0	2.246
−10.0	2.130	−10.0	2.426
−5.0	2.251	−5.0	2.527
0.0	2.368	−0.2	2.541
5.0	2.484		
10.0	2.605		

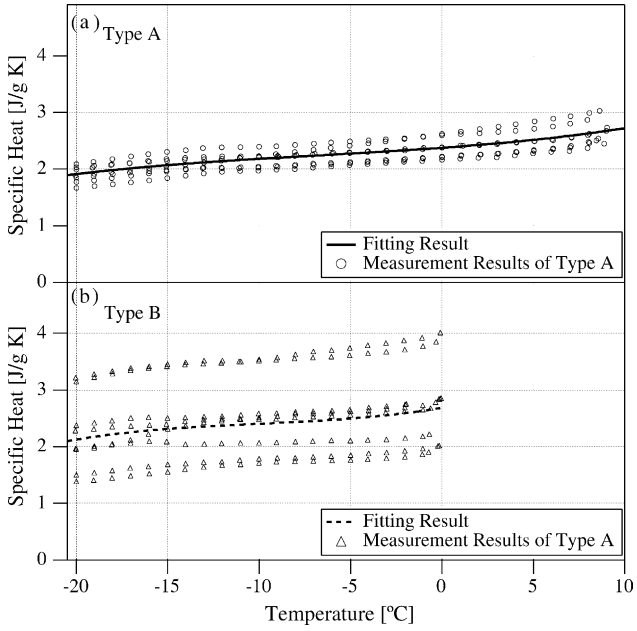

Fig. 3. Specific heats measurements and fitting results: (a) shows the type A and (b) shows the type B, respectively.

tion, it is more difficult to nucleate type B hydrate compared to type A, as indicated by the smaller number of crystals in the growth experiments, which is also consistent with type B having a lager hydration number. Fig. 1 shows that type A crystals grow larger than type B, but the latter crystals grow into polycrystalline aggregates of small, thin crystals. Therefore, since it is formed more easily, for industrial applications, it may be better to use type A. These thermophysical property results can be used for heat calculation of the equipment for gas separation or other industrial applications.

4. Conclusions

Thermal and thermodynamic properties of tetra-*n*-butyl ammonium bromide (TBAB) semiclathrate hydrate including their phase diagram have been measured. Two types of TBAB hydrates formed over the concentration range from 0 to 45%. It was determined that type A semiclathrate hydrate has a hydration number of 26.0, a 40 wt.% congruent melting point of 12 °C, and a eutectic point at 4.5 wt.%. The type B semiclathrate hydrate has a hydration number of 38.0, and a 38 wt.% congruent melting point of 9.9 °C. We did not detect a eutectic point for type B. The measured latent heat of type A was 193.18 ± 8.52 J/g and type B was 199.59 ± 5.28 J/g. We also measured the semiclathrate hydrate specific heats at various temperatures. These thermophysical properties should be useful for industrial applications of this material.

References

[1] Y. Nagano, M. Sakiyama, J. Phys. Chem. 92 (1988) 5823.
[2] J.A. Burns, R.E. Verrall, Thermochim. Acta 9 (1974) 277–287.
[3] T.G. Coker, J. Ambrose, G.J. Janz, J. Am. Chem. Soc. 92 18 (1970) 5293–5297.
[4] S. Fukushima, S. Takao, H. Ogoshi, H. Ida, S. Matsumoto, T. Akiyama, T. Otsuka, NKK Technical Report 166 (1999) pp. 65–70, in Japanese.
[5] Y. Wen, In Water and Aqueous Solutions, Wiley-Interscience, New York, 1972.
[6] W. Shimada, T. Ebinuma, H. Oyama, Y. Kamata, S. Takeya, T. Uchida, J. Nagao, H. Narita, JJAP 42 2A (2003) L129–131.
[7] Y. Kamata, H. Oyama, W. Shimada, T. Ebinuma, S. Takeya, T. Uchida, J. Nagao, H. Narita, JJAP 43 1 (2004) 362–365.
[8] H. Oyama, T. Ebinuma, W. Shimada, S. Takeya, T. Uchida, J. Nagao, H. Narita, Can. J. Phys. 81 (2003) 485–492.
[9] W. Shimada, T. Ebinuma, H. Oyama, S. Takeya, T. Uchida, J. Nagao, H. Narita, Proceedings of the Fourth International Conference on Gas Hydrates 1, (2002) 557–560.